MRS Communications (2017), 7, 938–946
© Materials Research Society, 2017
doi:10.1557/mrc.2017.121

MRS Communications

Research Letter

Achieving antimicrobial activity through poly(*N*-methylvinylimidazolium) iodide brushes on binary-grafted polypropylene suture threads

F. López-Saucedo, G.G. Flores-Rojas, and **E. Bucio,** Department of Radiation Chemistry and Radiochemistry, Instituto de Ciencias Nucleares, Universidad Nacional Autónoma de México, Circuito Exterior, Ciudad Universitaria, CDMX 04510, México
C. Alvarez-Lorenzo and **A. Concheiro,** Department of Pharmacology, Pharmacy, and Pharmaceutical Technology, R+DPharma Group (GI-1645), Facultad de Farmacia, Universidade de Santiago de Compostela, Santiago de Compostela 15782, España
O. González-Antonio, Department of Organic Chemistry, Facultad de Química, Universidad Nacional Autónoma de México, Ciudad Universitaria, CDMX 04510, México

Address all correspondence to F. López-Saucedo and E. Bucio at **felipelopezsaucedo@gmail.mx**; **ebucio@nucleares.unam.mx**

(Received 29 September 2017; accepted 16 October 2017)

Abstract

Harnessing the properties of imidazolium species, antimicrobial activity against Gram-negative and Gram-positive bacteria was attained by binary-grafting 2-hydroxyethyl methacrylate (HEMA) or *N*-isopropylacrylamide, followed by *N*-vinylimidazole onto polypropylene (PP) monofilaments (sutures) using ^{60}Co γ-rays. Ulterior functionalization with methyl iodide was carried out to endow brushes with antimicrobial activity on the PP surface. The PP-grafted sutures were characterized by means of Fourier-transform infrared spectroscopy attenuated total reflection, scanning electron microscopy, differential scanning calorimetry, and thermogravimetric analysis, and regarding the mechanical properties and the responsiveness to pH and temperature. Tests were performed on *Escherichia coli* and *Staphylococcus aureus* achieving large inhibition zones.

Introduction

There are currently a wide variety of polymers that exhibit specific characteristics of thermal and chemical stability, ductility, hardness, strength, elasticity, etc., which makes them useful in the manufacture of many products from daily use to highly specialized applications.[1] In this regard, materials that modify their behavior in response to a small change of their environment, e.g. temperature, pH, light, electricity, or magnetism are receiving increasing interest.[2] To achieve multi-responsiveness grafting, blends, or composites that combine two or more different polymer blocks are usually required.[3] Stimuli-responsive materials already find a variety of applications and quite different examples can be found in the literature.[4,5]

In the biomedical field, stimuli-responsive materials have open the possibility of developing: (a) biosensors that monitor in real time the health conditions of the patients for a more accurate diagnosis; (b) drug dosage forms and nanocarriers that can precisely regulate the release as a function of tiny changes in the cells environment; and (c) theranostic devices that perform diagnosis, therapy and monitoring functions in a single entity.[6,7] Additionally, implantable medical devices that typically exhibit inert behavior (e.g. prosthesis, sutures, catheters, etc.) may strongly benefit from responsive polymers that may pave the way for the design of personalized delivery systems and medical devices, which regulate the adhesion control of host cells and microorganisms or allow for a prolonged site-specific release of therapeutic agents.

In the case of medical devices, grafting of responsive polymers onto the surface is a suitable option to communicate novel performances.[8,9] The growth of the polymer chain can occur "from" the surface of the device, or a preformed polymer can be grafted "to" the device. In either case, the grafting may be triggered using chemical initiators or radiation [i.e. γ[10] or ultraviolet[11]], and it can occur at selected portions or regions of the device[12] generating materials with tailored surface or bulk. Polypropylene (PP) is a common component of medical devices,[13] particularly in suture threads, as well as of other wide variety of products for industrial processes and final consumers. Polyvinylimidazole (PNVIm) is a pH-responsive polymer with bacteriostatic properties, which may help to prevent health-care-associated infections.[14] Attempts to graft *N*-vinyl imidazole (NVIm) onto an aliphatic substrate, such as PP, usually leads to low yields,[15] hindering the full development of NVIm properties. Indeed, to provide antimicrobial features, PNVIm at low-grafting levels has been exploited to endow PP sutures with reversible binding points for a variety of antimicrobial drugs.[16] Antimicrobial surfaces that rely on hybrid materials and avoid the use of antibiotic molecules are receiving increasing attention as a way of minimizing the risk of triggering resistances.[17,18] Compared with other techniques for surface functionalization, radiation chemistry has the advantage of endowing the material surface with covalently bonded contact-killing polymers under milder conditions that can be easily scaled-up.[10]

https://doi.org/10.1557/mrc.2017.121 Published online by Cambridge University Press

The aim of this work was to implement a grafting approach that can improve the yield of PNVIm onto PP monofilaments. To do that, first γ-ray exposed PP monofilaments were treated with acrylic monomers to create brushes of hydrophilic 2-hydroxyethyl methacrylate (HEMA) or temperature-responsive *N*-isopropylacrylamide (NIPAAm).[19] The brushes served in a second step as support for the grafting of NVIm. Computational studies were carried out to gain an insight into the radical species that are thermodynamically favored and involved into the mechanism of grafting polymerization. Computational studies have been applied to screen functional monomers regarding their interactions with drugs,[20] to predict the properties of biomaterials and the biologic responses,[21] or to simulate radiation transport through biomaterial mimicking human tissues.[22] There is an increasing interest in applying computational modeling to the study of the thermodynamics and kinetics of different radical species as a tool to predict polymerization mechanisms and architecture of the resultant polymers.[23] However, the studies on binary grafting are still scarce,[24] and thus one of our aims is to shed light on the energy of formation of radicals that may be involved in the propagation reaction during NVIm grafting onto PP-*g*-HEMA and PP-*g*-NIPAAm.

Responsiveness to pH and temperature was measured as an index of the success of the grafting process. Series of the two binary grafted copolymers (PP-*g*-HEMA)-*g*-NVIm and (PP-*g*-NIPAAm)-*g*-NVIm were characterized using Fourier-transform infrared spectroscopy attenuated total reflection (FTIR-ATR), scanning electron microscopy (SEM), differential scanning calorimetry (DSC), thermogravimetric analysis (TGA), and recording the mechanical properties. Additional studies were cytocompatibility and antimicrobial against both Gram-negative (*Escherichia coli*) and Gram-positive (*Staphylococcus aureus*) bacteria, using the samples with and without quaternization of imidazole groups with methyl iodide (MeI) as an enhancer of antimicrobial activity without compromising cytocompatibility.

Experimental

Materials

Reagents methyl iodide (99%), NIPAAm (97%), HEMA (98%), and NVIm (99%) were purchased from Aldrich Chemical Co. (St. Louis, MO, USA). NIPAAm was purified by crystallization with toluene/hexane 50/50 vol%. Monomers HEMA and NVIm were purified by vacuum distillation. PP monofilaments (Atramat 1 USP suture threads) were supplied by Internacional Farmacéutica Co (Mexico). Ethanol, toluene, *n*-hexane, boric acid, citric acid, trisodium orthophosphate 12 H_2O, and phosphate buffer solution (PBS) were from Baker (Mexico City, Mexico). Fibroblast cells (BALB/3T3; ATCC CCl-163TM), *S. aureus* (ATCC 25923) and *E. coli* (ATCC 25922) were from the American Type Culture Collection (Manassas, VA, USA). Dulbecco's Modified Eagle's Medium (DME)/Ham's Nutrient Mixture F-12 (DMEM F12 HAM), fetal bovine serum (FBS) and Müller-Hinton agar were purchased from Aldrich Chemical Co. (St. Louis MO, USA).

Synthesis of PP-g-HEMA and PP-g-NIPAAm

PP monofilaments (10 cm length) were weighed, and placed into glass ampoules, and exposed to γ-rays using a ^{60}Co source (Gammabeam 651-PT) in the presence of oxygen from air with different irradiation doses.

After the pre-irradiation, 6 mL of NIPAAm or HEMA solution in toluene with a concentration 1.5 and 1 mol L^{-1} was added to the ampoules, which were then degassed by repeated freeze–thaw cycles (three times per 10 min), sealed at vacuum and placed in a water bath at a given temperature and time (Table S1). Once the reaction time was completed, the copolymers PP-*g*-HEMA and PP-*g*-NIPAAm were washed in a mixture of water/ethanol 50/50 vol%, under stirring for 24 h. The product was dried in a vacuum oven at 60 °C for 24 h. Toluene was chosen because it is a good solvent for the monomers, swells PP without dissolution and could be easily removed with ethanol.

Grafting percentage was calculated from the weight of pristine (W_0) and grafted (W_g) monofilament as follows in Eq. (1):

$$\text{Grafting (\%)} = 100\,[(W_g - W_0)/W_0]. \quad (1)$$

Synthesis of binary grafting with NVIm

The second grafting with NVIm was carried out using pieces of pristine PP, and PP-*g*-HEMA and PP-*g*-NIPAAm with different grafting degree. The monofilaments were weighed and placed into glass ampoules with NVIm solutions (6 mL) with different concentrations of toluene. The ampoules were degassed by repeated freeze–thaw cycles (three times per 10 min), sealed at vacuum and irradiated at different doses. Afterwards the glass ampoules were opened, and the grafted monofilaments were washed and dried using the procedure described above. Grafting degree was calculated according to Eq. (1). Reaction conditions of NVIm grafting are specified in Table S2.

Computational methods

All computational calculations were carried out on the Gaussian 09 software and consisted of the following:

I. An oligomeric portion of the graft was calculated inferring the electronic and chemical structure remain considerably constant along the polymeric graft as the spectroscopic analysis evidenced, given linear polymeric chains in the grafting polymerization;[25] this helps considering an oligomeric portion to be representative of a macromolecular section.
II. PM6 and PM3 semiempirical methods were applied to perform the calculations for NIPAAm and HEMA, respectively, knowing previous evidence of this kind of computational approach have been used for such systems.[26]
III. Based on the importance of including in a theoretical study the solvent for the polymerization reaction as reported by De Sterck et al.,[27] the PCM (Polarizable Continuum Model) was used.

https://doi.org/10.1557/mrc.2017.121 Published online by Cambridge University Press

IV. Through a chemically intuitive criterion, the four most likely radical species for each system were considered and their total energies were calculated, establishing thus what species would be thermodynamically favored and more probable to start the reaction with the imidazole derivative.

Swelling tests

Pieces (10 cm) of grafted sutures were placed in flasks containing distilled water. The swelling test was carried out at 25 °C and the degree of swelling was monitored weighting the suture pieces at different time intervals up to 24 h. Additionally, swelling of PP-*g*-NIPAAm copolymers was measured at different temperatures from 6 to 55 °C for determination of lower critical solution temperature (LCST). Critical pH of (PP-HEMA)-*g*-NVIm and (PP-*g*-NIPAAm)-*g*-NVIm was determined to record the swelling in phosphate buffers covering from pH 2 to 12. The degree of swelling was calculated as follows in Eq. (2):

$$\text{Swelling}\ (\%) = 100\ [(W_s - W_d)/W_d], \qquad (2)$$

where W_s and W_d represent the weights of the swelled and the dried grafted suture, respectively.

The data were processed to calculate LCST and pH critical point using Boltzmann function in Origin Pro 9 software.

Characterization of grafted sutures

FTIR-ATR spectra of pristine and modified sutures were recorded on a Perkin-Elmer Spectrum 100 spectrometer (Perkin Elmer Cetus Instruments, Norwalk, CT) with 16 scans. Thermal decomposition was monitored by TGA under a nitrogen atmosphere from 25 to 800 °C at a heating rate of 10 °C min^{-1} in a TGA Q50 (TA Instruments, New Castle, DE). DSC analysis were carried out under nitrogen atmosphere using a DSC 2010 calorimeter (TA Instruments, New Castle, DE) from 25 to 350 °C at a heating rate of 10 °C min^{-1}. SEM images of the surface and transversal cut of the filaments after being swollen in water and freeze-dried were recorded using Zeiss EVO LS15 (Germany) apparatus.

Tensile stress–strain plots and force at failure

Tests were carried out as described previously using a computer-controlled TA-TX Plus Texture Analyzer (Stable Micro Systems Ltd., Surrey, UK) and 30 kg load cell.[15] In each test, a piece of suture was firmly fixed in the lower and the upper grips (initial gap 55 mm). Then, the stress–strain (elongation) curve of the suture was recorded while subjected to uniaxial tension at a rate of 0.5 mm s^{-1} until failure. The tensile stress and elongation at rupture and the work of resilience (area under the curve until rupture) were calculated.[28]

Quaternization: formation of methylimidazolium iodide

Pieces of PP and the grafted monofilaments (PP-*g*-HEMA)-*g*-NVIm and (PP-*g*-NIPAAm)-*g*-NVIm were placed inside ampoules containing MeI solutions (5, 20, 50, and 100 vol%) in toluene. The ampoules were sealed and incubated at 40 °C for 24 h. Then, the monofilaments were soaked in toluene and dried in a vacuum oven at 60 °C for 24 h. Samples were stored at room temperature.

Cytocompatibility

Sutures were cut in 5 mm length pieces and immersed in PBS overnight. Then, they were sterilized under UV light for 30 min. Balb/3T3 were seeded in 96-well plates (20000 cells/well in 200 µL of complete culture medium containing 89% DMEM F12 HAM, 10% FBS and 1% penicillin/streptomycin) and allowed to attach for 24 h in a humidified atmosphere with 5% CO_2, 90% RH at 37 °C. Then, suture pieces were placed individually in the wells and cultured for 48 h. Cells cultured in complete culture medium without suture were used as negative control. At 24 and 48 h of culture, the medium was discarded and 100 µL of fresh medium was placed in each well. Then, 10 µL of 10× AlamarBlue® cell viability reagent (ThermoFisher, USA) were added to each well and incubated in darkness at 37 °C for 4 h. Finally, the absorbance was read at 570 nm in a microplate reader (BioRad model 680, USA). Absorbance of the negative control was referred as 100% viability and the cell viability recorded in the presence of the suture pieces was referred to that value.

Microbiological tests

Petri plates containing Müller-Hinton agar were seeded with *S. aureus* ATCC 25923 ($2.8{\cdot}10^8$ CFU mL^{-1}) or *E. coli* ATCC 25922 ($3.4{\cdot}10^8$ CFU mL^{-1}). Pieces (1 cm) of pristine PP and all grafted monofilaments, as such and after treatment with MeI were soaked overnight in sterile PBS, dried and then placed in the plates. Then, the plates were incubated at 37 °C for 24 h and the zones of inhibition were measured (perpendicularly to the monofilament).

Results and discussion

Modification of PP by means of grafting of HEMA, NIPAAm, or NVIm in separate has been previously reported.[15] The present work is focused on binary grafting in which PP was first grafted with either HEMA or NIPAAm in order that the grafted chains facilitated the grafting of NVIm in a subsequent step. The obtained (PP-HEMA)-*g*-NVIm and (PP-*g*-NIPAAm)-*g*-NVIm were then characterized in detail.

Grafting

PP-*g*-HEMA and PP-*g*-NIPAAm were prepared covering a wide range of grafting percentages, these intermediates are important because the direct grafting of NVIm onto PP is difficult and the NVIm grafting ratio is decisive in the antibacterial activity. After simultaneous γ irradiation of NVIm in the second step (direct method) some tendencies were found, firstly the amount of NVIm grafted was positively correlated with the degree of HEMA or NIPAAm in the first step [Fig. 1(a)]. The reaction conditions were tuned at low-dose exposure and

https://doi.org/10.1557/mrc.2017.121 Published online by Cambridge University Press

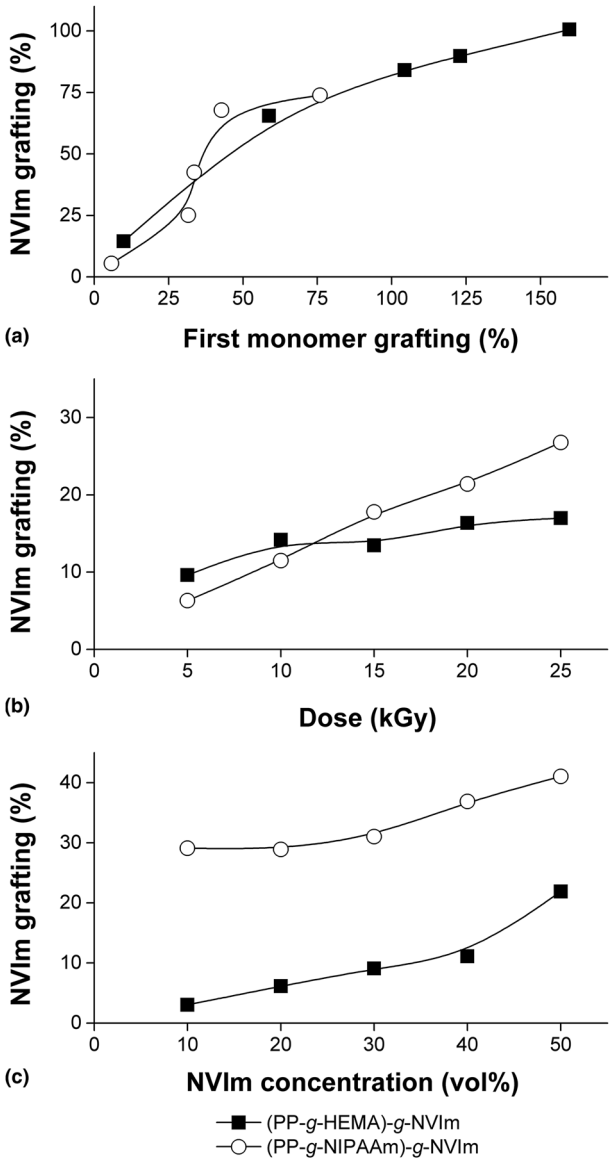


Figure 1. Grafting studies of NVIm: PP-*g*-HEMA and PP-*g*-NIPAAm. (a) Influence of the initial grafting percentage, total dose of 25/30 kGy and 50 vol % NVIm in toluene; (b) effect of absorbed dose during NVIm grafting onto PP-*g*-HEMA (19%) and PP-*g*-NIPAAm (34%) (first step grafting dose was 15 kGy) using 50 vol% NVIm in toluene; (c) effect of NVIm concentration during grafting onto (PP-*g*-HEMA) (51%) and PP-*g*-NIPAAm (53%) for total dose of 20/20 kGy for each grafting.

a total percentage of grafting below 100% to keep mechanical properties like pristine PP. Otherwise, monofilament structure and the mechanical properties became altered and its functionality spoilt. For this reason, PP-*g*-HEMA and PP-*g*-NIPAAm monofilaments were exposed to absorbed doses in the range of 5–25 kGy [Fig. 1(b)]. Under these conditions, the grafting of NVIm from PP-*g*-HEMA (19%) attained values of 10–17%, while from PP-*g*-NIPAAm (34%) varied between 6% and 27%. For a fix dose of 20 kGy, the effect of NVIm/toluene vol/vol ratio of the grafting percentage was evaluated, as the NVIm concentration increased from 10 to 50 vol% the percentage of grafting increased from 3% to 22% for PP-*g*-HEMA (51%) and from 29% to 41% for PP-*g*-NIPAAm (53%) [Fig. 1(c)]. Thus, a positive correlation of the grafting percentage on the NVIm concentration was also found.

Overall, these findings indicate that the first grafting of PP with HEMA and NIPAAm chains notably favors the subsequent grafting of NVIm, and it is possible to prepare monofilaments having similar percentages in both grafted polymers. Also, a small increment in the diameter of the monofilaments functionalized with higher grafting percentages was observed (Table S3), which suggests that the grafting mainly occurred on the surface. To gain an insight into this point, SEM images of the surface and transversal cut of the threads were recorded. The images of binary grafts with low percentages of grafting [Fig. 2(a)] maintained the smooth surface of pristine PP monofilaments [Figs. 2(b) and 2(c)]. Differently, highly grafted monofilaments showed deposits on the surface, in the case of (PP-*g*-HEMA)-*g*-NVIm (104/84%) [Figs. 2(d) and 2(e)], and grafting in bulk was observed for (PP-*g*-NIPAAm)-*g*-NVIm (76/74%) [Figs. 2(f) and 2(g)].

Computational study

Computational studies were carried out to identify the most likely radical species that could be formed on PP-*g*-HEMA and PP-*g*-NIPAAm and to compare their total energies. Computed energy values and structure of the different studied molecules are compared in Fig. 3. In the case of PP-*g*-NIPAAm, the radical species that would result in higher thermodynamic stability and, therefore, more plausible formation, was the one that has the radical located on the "*iso*propyl" portion of the terminal NIPAAm. Alpha and beta positions relative to the amide carbonyl (iii and ii, respectively) are 11.2 and 12.7 kcal mol^{-1} above the minimum-energy radical, rendering them too distant to be favored during the radical formation. The radical formed on the amidic nitrogen (i) would be the least probable entity to reach formation, since it requires 28.8 kcal mol^{-1} above the minimum. Molecular orbital contour plot shows that the lowest energy radical is stabilized via π-delocalization from the *iso*propyl through the amide, which is well known to be also π-delocalized, which yields the low-energy state as a result.

On the other hand, for PP-*g*-HEMA, the energetic of formation of radical species is quite different, showing a relative minimum when the radical is formed on the α position of the ester carbonyl. Nonetheless, it could not be ruled out that the α position from the ester oxygen and the alpha position from the hydroxyl group, with only 3.5 kcal mol^{-1} above the minimum, are also formed during the reaction (v and vi, respectively). The stabilization of the lowest energy radical species comes from the heavy contribution of the π-delocalization of the radical-bearing carbon and the two oxygen atoms from the ester system (see molecular orbital contour plot; Figure 3). An equally stabilizing delocalization would be expected in the other two near states. However, a non-negligible delocalization component is set by the hyperconjugation with the adjacent carbon–carbon

https://doi.org/10.1557/mrc.2017.121 Published online by Cambridge University Press

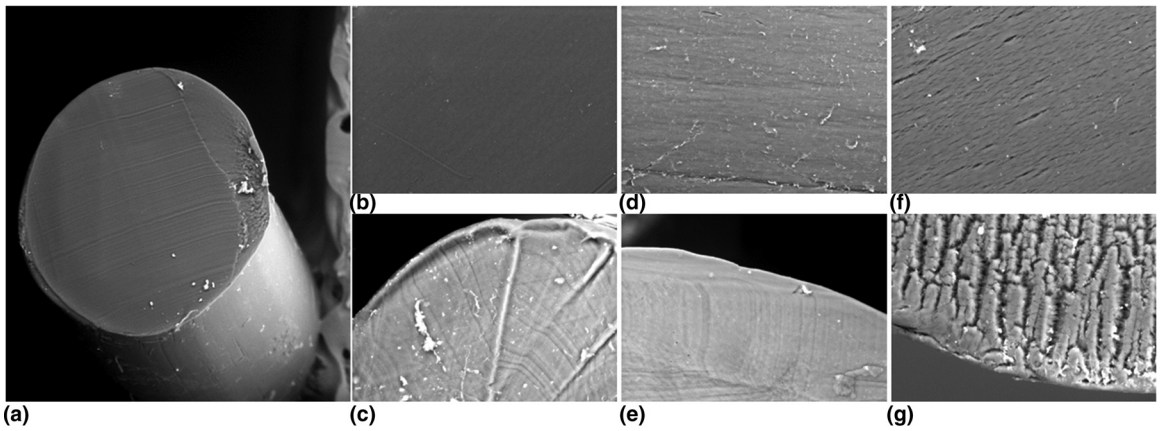


Figure 2. SEM images of (a) (PP-*g*-NIPAAm)-*g*-NVIm (6/5%) augmented 200×; surface (up) and transversal cut (down) respectively of: (b, c) pristine PP; (d, e) (PP-*g*-HEMA)-*g*-NVIm (104/84%);(f, g) (PP-*g*-NIPAAm)-*g*-NVIm (76/74%) augmented 1000×.

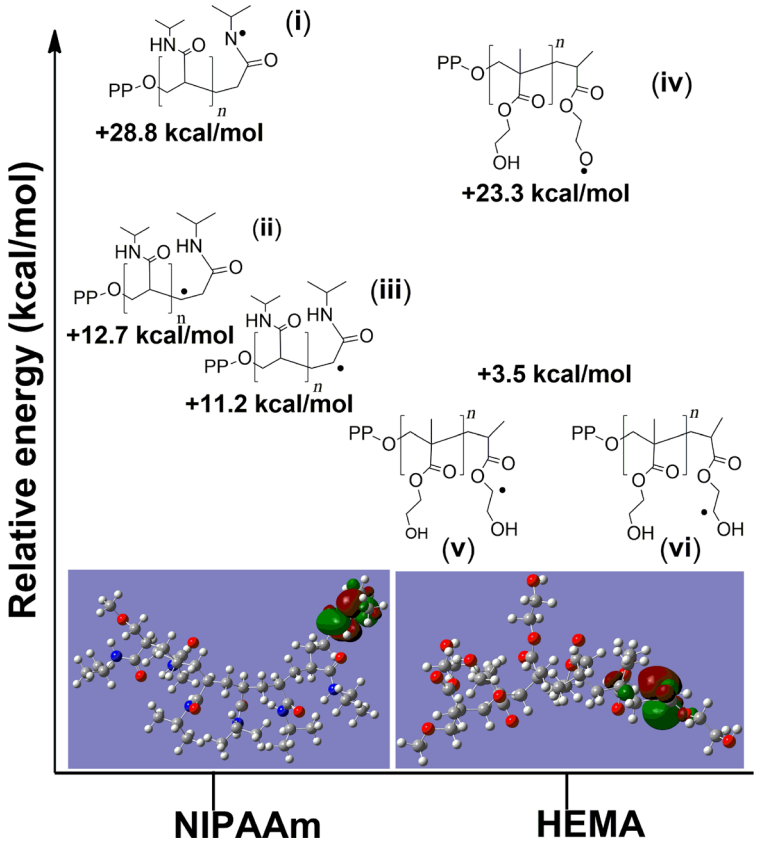


Figure 3. Calculated relative total energy for the most plausible radical species for both grafts and molecular orbital contour plots for the found minima; proposed NIPAAm (i, ii, iii), and HEMA (iv, v, vi) radical fragments.

bond (beta methylene from the ester and the quaternary carbon joining two monomers). This effect could be the chief selection rule to determine the favored position for the polymerization reaction, which differentiates the plausibility of formation for the two near species. The hydroxy-terminal radical (iv) in the HEMA graft is the one with the highest energy, 23.3 kcal mol^{-1} above the minimum, and thus the growth of PNVIm chain from this radical is not expected to occur.

https://doi.org/10.1557/mrc.2017.121 Published online by Cambridge University Press

Infrared spectroscopy

FTIR-ATR analysis of the single and binary grafted PP monofilaments allowed the identification of the characteristics bands of each polymer (Fig. 4). PP-*g*-HEMA had CO carbonyl bands at 1724 cm^{-1} and OH alcohol at 3397 cm^{-1}. The PP-*g*-NIPAAm spectrum showed the amide bands of CO carbonyl at 1646 cm^{-1} and the weak band of stretching NH at 3299 cm^{-1}. For comparison purposes, the spectrum of PP-*g*-NVIm was also recorded, and exhibited the bands of stretching of double bound CC and CN of imidazole ring at 1673 cm^{-1}, the aromatic CH stretching at 3109 cm^{-1}, and the characteristic pattern in the fingerprint region (1250–400 cm^{-1}).

The binary graft copolymers also showed similar fingerprint region, plus the bands typical of each polymer. Namely, in the spectrum of (PP-*g*-HEMA)-*g*-NVIm (123/90%) the main bands corresponded to CO at 1716 cm^{-1}, OH at 3386 cm^{-1}, aromatic CH at 3112 cm^{-1}, and aromatic ring at 1657 cm^{-1}. In the case of (PP-*g*-NIPAAm)-*g*-NVIm (34/43%), the main bands were due to CO at 1645 cm^{-1}, NH at 3363 cm^{-1}, and aromatic CH at 3108 cm^{-1}. The signals of NVIm were relatively more intense, which confirmed the predominance of the imidazole chains at the surface.

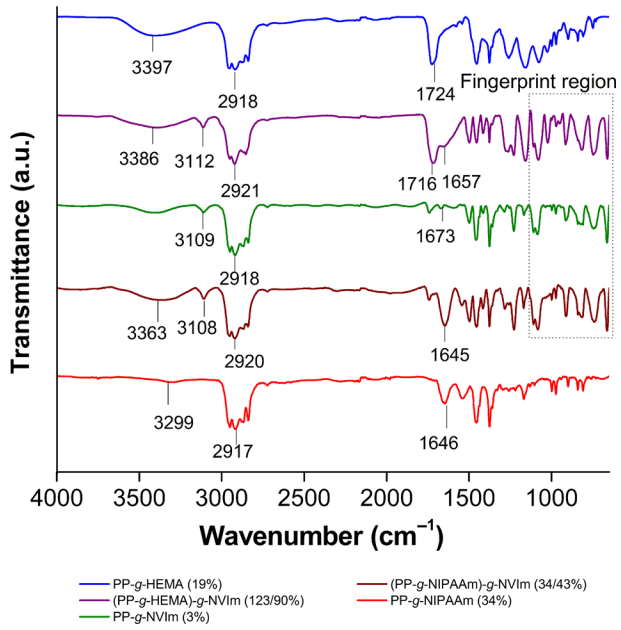


Figure 4. FTIR-ATR spectra. Functional groups are identified in each grafting.

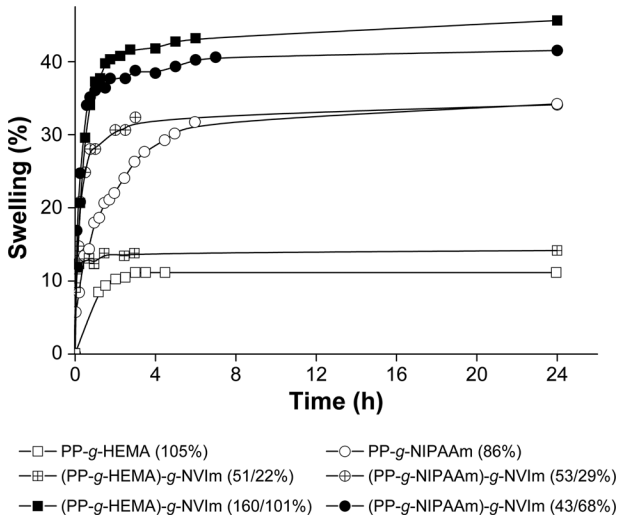


Figure 5. Swelling of PP-*g*-HEMA and PP-*g*-NIPAAm single grafts and the corresponding binary grafts in water at 25 °C.

Swelling

Compared with pristine PP monofilament that does not sorb water, grafted copolymers showed swelling in an aqueous

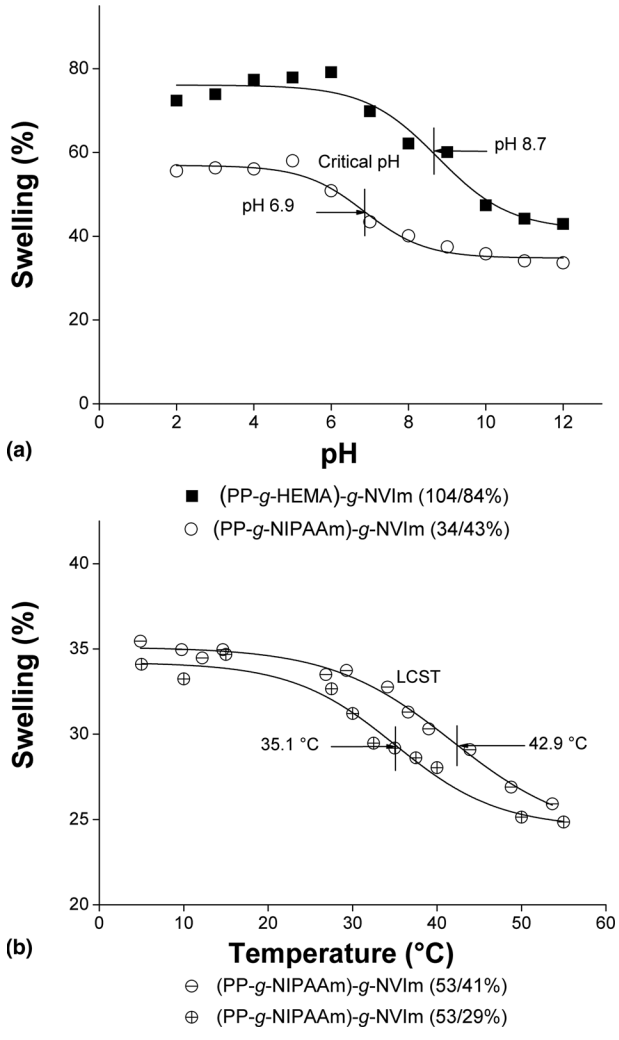


Figure 6. (a) Effect of pH on the swelling of binary grafts in phosphate buffers at 25 °C for 24 h. (b) Effect of temperature on the swelling of (PP-*g*-NIPAAm)-*g*-NVIm in water.

https://doi.org/10.1557/mrc.2017.121 Published online by Cambridge University Press

Table I. TGA values (weight loss, decomposition temperature, and char yield) and DSC (melting temperature) of monofilaments before and after single and binary grafting.

Monofilament	10 wt% loss (°C)	T_d (°C)	Char yield % (at 450 °C)	DSC T_m (°C)
Pristine PP	423.3	462.5	64.7	169.8
PP-*g*-NVIm (3%)	421.3	461.6	61.7	170.2
PP-*g*-NIPAAm (34%)	408.0	461.7	61.4	171.4
PP-*g*-HEMA (19%)	391.3	461.9	53.2	169.6
(PP-*g*-NIPAAm)-*g*-NVIm (34/43%)	215.9	224.7, 416.4, 458.9	33.9	174.4
(PP-*g*-HEMA)-*g*-NVIm (123/90%)	273.6	141.9, 326.6, 472.6	25.7	170.5

Td, Thermal decomposition.

medium (Fig. 5). The three grafted polymers evaluated possess hydrophilic groups in their structure,[29] and the interaction with water may depend on the linear/branched architecture of the chains and the environmental conditions (which may act as specific stimuli). All grafted monofilaments showed a quite rapid swelling and attained the equilibrium in less than 6 h at room temperature, corroborating the hypothesis that the grafting mainly took place at the surface.

PP-*g*-HEMA with a grafting percent as high as 104% only swelled 11%. Differently, after grafting of NVIm chains, the swelling of (PP-*g*-HEMA)-*g*-NVIm (51/22 and 160/101%) increased up to 15% and 45%, respectively. Similar behavior was found with PP-*g*-NIPAAm (86%) which swelled 31%, while (PP-*g*-NIPAAm)-*g*-NVIm (43/68%) did it above 40%.

Regarding temperature responsiveness, second grafting with NVIm shifted to higher values of the typical LCST of PNIPAAm (close to 30 °C) [Fig. 6(a)], as observed for other PNIPAAm networks.[19] As the content in NVIm increased the shift was more evident. For example, (PP-*g*-NIPAAm)-*g*-NVIm (53/29%) had a LCST of 35.1 °C, whereas for (PP-*g*-NIPAAm)-*g*-NVIm (53/41%) the LCST increased up to 42.9 °C.

All binary grafts (PP-*g*-HEMA)-*g*-NVIm and (PP-*g*-NIPAAm)-*g*-NVIm exhibited pH-responsiveness [Fig. 6(b)]. This property is endowed by the heteroaromatic ring of the imidazole group, which has a pKa of about 6.79.[30] In acid medium, this group is protonated and the polymer is highly hydrated; oppositely, the change to an alkaline environment caused the polymer loses its charge and thus the chain-collapse; consequently, a decrease in swelling occurs. The critical pH was shifted to higher values as the content in NVIm increased.

Thermal analysis and mechanical properties

In the DSC runs, all single and binary grafted sutures showed the typical melting band of PP with minor changes in melting temperature compared to pristine suture (Fig. S1). This finding suggests that the thermal stability of PP was not significantly altered. The TGA analysis revealed that the binary grafted copolymers started decomposition at lower temperature compared with pristine and singly grafted sutures (Fig. S2). The thermogram scan of binary grafts revealed multiple stages of decomposition for (PP-*g*-HEMA)-*g*-NVIm (123/90%) and (PP-*g*-NIPAAm)-*g*-NVIm (34/43%). These results (Table I) suggested different polymer composition per zone, this means PP is in the core, HEMA, or NIPAAm mainly are inner, and NVIm chains are at the surface.

Pristine PP monofilaments had tensile stress of 5.0 kg and the work of resilience was 24.7 kg·mm. Binary grafted monofilaments with low graft percentage (less than 50%) became brittle and the tensile stress decreased to 2.7–3.2 kg and the work of resilience to 5.0–10.0 kg mm. Differently, (PP-*g*-HEMA)-*g*-NVIm (104/84%) and (PP-*g*-NIPAAm)-*g*-NVIm (76/74%) monofilaments broke at shorter elongation, but the stress required was higher 6.0 and 5.2 kg, respectively, as well as the tensile stress 38.0 and 30.6 kg·mm.

Cytocompatibility and antimicrobial activity

The next step was to confirm that the binary grafting did not alter the excellent cytocompatibility of the starting monofilaments (probed by their long use as sutures). The experiments were carried out with fibroblast cells (Balb 3T3 cells) which are particularly sensitive to leaching substances from medical devices that might be toxic. Sutures with extreme contents in grafted copolymers were tested. As shown in Fig. 7(a), cell viability was above 80% after direct contact with any of the binary grafted sutures either for 24 or 48 h. This finding indicates that the binary grafted sutures are cytocompatible disregarding the grafting percentage. Importantly, treatment with MeI for PNVIm quaternization followed by intense washing to remove unreacted species did not alter the cytocompatibility of the monofilaments. This result is in good agreement with previous studies.[31]

MeI readily reacted with the imidazole groups of the grafted NVIm forming methylimidazolium iodide derivative that reinforce the antimicrobial activity of the monofilaments. Pieces of pristine PP and all grafted monofilaments, as such and after treatment with MeI, were challenged against *S. aureus* and *E. coli* strains. The pristine PP sutures exposed or not to MeI did not inhibit bacteria growth neither the binary grafted

https://doi.org/10.1557/mrc.2017.121 Published online by Cambridge University Press

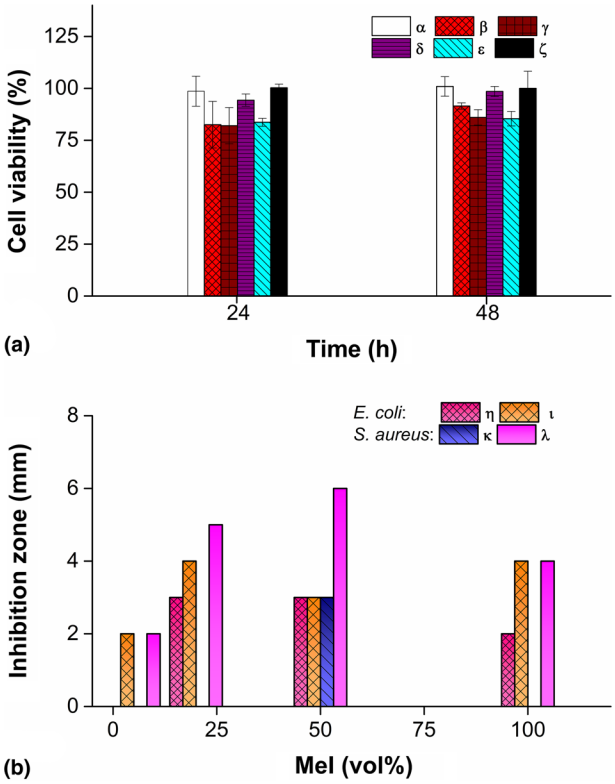


Figure 7. (a) Cell viability: (α) PP, (β) (PP-*g*-NIPAAm)-*g*-NVIm (6/5%), (γ) (PP-*g*-NIPAAm)-*g*-NVIm (76/74%), (δ) (PP-*g*-HEMA)-*g*-NVIm (10/14%), (ε) (PP-*g*-HEMA)-*g*-NVIm (104/84%), (ζ) negative control. (b) Inhibition zone. *E. coli*: (η) (PP-*g*-NIPAAm)-*g*-NVIm (20/22%), (ι) (PP-*g*-HEMA)-*g*-NVIm (36/22%); *S. aureus*: (κ) (PP-*g*-NIPAAm)-*g*-NVIm (20/22%), (λ) (PP-*g*-HEMA)-*g*-NVIm (36/22%).

monofilaments (PP-*g*-HEMA)-*g*-NVIm and (PP-*g*-NIPAAm)-*g*-NVIm, which clearly indicate that none antimicrobial substance was released to the agar, although anti-adhesion activity could not be discarded. Differently, after treatment with MeI all binary grafts showed remarkable ability to cause inhibition zones [Fig. 7(b)]. The inhibition zone caused by quaternary methylimidazolium (PP-*g*-HEMA)-*g*-NVIm (36/22%) became progressively greater as the concentration of MeI increased from 5 to 50 vol%; the inhibition zone in *S. aureus* augmented from 2 to 6 mm and in *E. coli* from 2 to 4 mm. Exposure to higher MeI concentration did not improve further the antimicrobial effect. In the case of quaternary methylvinylimidazolium (PP-*g*-NIPAAm)-*g*-NVIm (20/22%), the greater inhibition zones (3 mm) were observed in *S. aureus* and *E. coli* after treatment with 50 vol% MeI in toluene.

The differences in antimicrobial activity can be explained in terms of quaternization degree. Under mild conditions (40 °C) the reaction proceeds best when the matrix swells and this occurs using toluene as solvent. Therefore, exposition of the binary grafted monofilaments to MeI 100vol% (i.e., in the absence of toluene) only caused superficial derivatization. Oppositely, when the reaction was carried out using 5 vol% MeI, the quaternization was incomplete. These findings indicate that the formation of imidazolium iodide requires a fine balance of the ratio of the solvent used to swell the matrix and the MeI required for the reaction with imidazole groups.

Conclusions

Grafting of NVIm onto PP can be notably improved when PP-*g*-HEMA and PP-*g*-NIPAAm are used as intermediates, compared with the direct grafting onto the pristine PP. The computational modeling indicates that the grafting of NVIm from PP-*g*-NIPAAm is likely to occur through the *iso*propyl terminal fragment of the polymer, while in PP-*g*-HEMA the path is less clear, although stereoelectronic calculations suggest that the grafting initiates from the alpha position of the carbonyl ester group. Functionalization with NVIm endows PP monofilaments with pH-responsiveness; (PP-*g*-NIPAAm)-*g*-NVIm exhibiting both pH- and temperature-responsiveness. Relevantly, an adequate balance of MeI concentration is required to attain sufficient quaternary derivative. All binary grafted monofilaments show good cytocompatibility and can inhibit the growth of both Gram-negative (maximum inhibition zone 4 mm) and Gram-positive (maximum inhibition zone 6 mm) bacteria after quaternization. Overall, the designed antibacterial biomaterial may be useful for the development of new non-absorbable sutures.

Supplementary material

The supplementary material for this article can be found at https://doi.org/10.1557/mrc.2017.121

Acknowledgments

This work was supported by DGAPA-UNAM under Grant IN201617 (Mexico); MICINN under Grant SAF2014-52632-R (Spain); FEDER. F.L.S. thanks CONACyT for the doctoral scholarship 409872/ 290649 (CVU/ scholarship holder). The authors thank B. Leal and M. Cruz from ICN-UNAM for technical assistance and B. Magariños from USC for help with microbiological tests.

References

1. P.-F. Cao, J.D. Mangadlao, and R.C. Advincula: Stimuli-responsive polymers and their potential applications in oil-gas industry. *Polym. Rev.* **55**, 706 (2015).
2. S. Guragain, B.P. Bastakoti, V. Malgras, K. Nakashima, and Y. Yamauchi: Multi-stimuli-responsive polymeric materials. *Chem. A, Eur. J.* **21**, 13164 (2015).
3. Z.Q. Cao and G.J. Wang: Multi-stimuli-responsive polymer materials: particles, films, and bulk gels. *Chem. Rec.* **16**, 1398 (2016).
4. J. Akimoto, M. Nakayama, K. Sakai, M. Yamato, and T. Okano: Synthesis of terminal-functionalized thermoresponsive diblock copolymers using biodegradable macro-RAFT agents. *Polym. J.* **45**, 233 (2012).
5. O. Sedláček, P. Černoch, J. Kučka, R. Konefal, P. Štěpánek, M. Vetrík, T. P. Lodge, and M. Hrubý: Thermoresponsive polymers for nuclear medicine: which polymer is the best? *Langmuir* **32**, 6115 (2016).
6. S. Liu, R. Maheshwari, and K.L. Kiick: Polymer-based therapeutics. *Macromolecules* **42**, 3 (2009).
7. C. Alvarez-Lorenzo and A. Concheiro: Smart drug delivery systems: from fundamentals to the clinic. *Chem. Commun.* **50**, 7743 (2014).

https://doi.org/10.1557/mrc.2017.121 Published online by Cambridge University Press

8. C. Feng, Y. Li, D. Yang, and J. Hu: Well-defined graft copolymers: from controlled synthesis to multipurpose applications. Chem. *Soc. Rev.* **40**, 1282 (2011).
9. M.A.C. Stuart, W.T.S. Huck, J. Genzer, M. Muller, C. Ober, M. Stamm, G. B. Sukhorukov, I. Szleifer, V.V. Tsukruk, M. Urban, F. Winnik, S. Zauscher, I. Luzinov, and S. Minko: Emerging applications of stimuli-responsive polymer materials. *Nat. Mater.* **9**, 101 (2010).
10. C. Alvarez-Lorenzo, E. Bucio, G. Burillo, and A. Concheiro: Medical devices modified at the surface by g-ray grafting for drug loading and delivery. *Expert Opin. Drug Deliv.* **7**, 173 (2010).
11. C. Decker: The use of UV irradiation in polymerization. *Polym. Int.* **45**, 133 (1998).
12. S. Minko: Chapter 93 Grafting on solid surfaces: "grafting to" and "grafting from" methods. In *Polymer Surfaces and Interfaces: Characterization, Modification and Applications*, edited by M. Stamm (Springer, Berlin, 2008), p. 215.
13. M.F. Maitz: Applications of synthetic polymers in clinical medicine. *Biosurf, Biotribol.* **1**, 161 (2015).
14. H. Caner, E. Yilmaz, and O. Yilmaz: Synthesis, characterization and antibacterial activity of poly(N-vinylimidazole) grafted chitosan. *Carbohydr. Polym.* **69**, 318 (2007).
15. F. López-Saucedo, C. Alvarez-Lorenzo, A. Concheiro, and E. Bucio: Radiation-grafting of vinyl monomers separately onto polypropylene monofilament sutures. *Radiat. Phys. Chem.* **132**, 1 (2017).
16. B. Gupta, N. Anjum, S.K.H. Gulrez, and H. Singh: Development of antimicrobial polypropylene sutures by graft copolymerization. II. Evaluation of physical properties, drug release, and antimicrobial activity. *J. Appl. Polym. Sci.* **103**, 3534 (2007).
17. T. Modjinou, H. Rodriguez-Tobias, G. Morales, D.-L. Versace, V. Langlois, D. Grande, and E. Renard: UV-cured thiol–ene eugenol/ZnO composite materials with antibacterial properties. *RSC Adv.* **6**, 88135 (2016).
18. H. Rodríguez-Tobías, G. Morales, A. Ledezma, J. Romero, R. Saldívar, V. Langlois, E. Renard, and D. Grande: Electrospinning and electrospraying techniques for designing novel antibacterial poly(3-hydroxybutyrate)/zinc oxide nanofibrous composites. *J. Mater. Sci.* **51**, 8593 (2016).
19. B.A. Humphreys, J.D. Willott, T.J. Murdoch, G.B. Webber, and E.J. Wanless: Specific ion modulated thermoresponse of poly(N-isopropylacrylamide) brushes. *Phys. Chem. Chem. Phys.* **18**, 6037 (2016).
20. C. Lei, L.Y. Kee, M. Yanawut, T.K. Soo, L.V. Sanghiran, and R.N. Abd: Synthesis, characterization, and theoretical study of an acrylamide-based magnetic molecularly imprinted polymer for the recognition of sulfonamide drugs. *e-Polymers* **15**, 141 (2015).
21. A.D. Costache, J. Ghosh, D.D. Knight, and J. Kohn: Computational methods for the development of polymeric biomaterials. *Adv. Eng. Mater.* **12**, B3 (2010).
22. C. Wojnecki and S. Green: A computational study into the use of polyacrylamide gel and A-150 plastic as brain tissue substitutes for boron neutron capture therapy. *Phys. Med. Biol.* **46**, 1399 (2001).
23. E. Mavroudakis, D. Cuccato, and D. Moscatelli: On the use of quantum chemistry for the determination of propagation, copolymerization, and secondary reaction kinetics in free radical polymerization. *Polymers* **7**, 1789 (2015).
24. Y.A. Anisimov, M.A. Danilenko, and Y.N. Anisimov: Copolymerization of modified oligoesteracrylates with oligomeric butadiene rubber. *Russ. J. Appl. Chem.* **86**, 289 (2013).
25. E.A. Morales-Wiemer, J. Macossay, and E. Bucio: Radiation grafting of N, N'-dimethylacrylamide and 2-hydroxyethylmethacrylate onto polypropylene films by one step method. *Radiat. Phys. Chem.* **84**, 166 (2013).
26. L.D. Marestoni, A. Wong, G.T. Feliciano, M.R.R. Marchi, C.R.T. Tarley, and M.D.P.T. Sotomayor: Semi-empirical quantum chemistry method for pre-polymerization rational design of ciprofloxacin imprinted polymer and adsorption studies. *J. Braz. Chem. Soc.* **27**, 109 (2016).
27. B. De Sterck, R. Vaneerdeweg, F. Du Prez, M. Waroquier, and V. Van Speybroeck: Solvent effects on free radical polymerization reactions: the influence of water on the propagation rate of acrylamide and methacrylamide. *Macromolecules* **43**, 827 (2010).
28. P.P. Caimmi, M. Sabbatini, L. Fusaro, A. Borrone, and M. Cannas: A study of the mechanical properties of ePTFE suture used as artificial mitral chordate. *J. Card. Surg.* **31**, 498 (2016).
29. K.S. Oh, S.K. Han, Y.W. Choi, J.H. Lee, J.Y. Lee, and S.H. Yuk: Hydrogen-bonded polymer gel and its application as a temperature-sensitive drug delivery system, Biomaterials. *Biomaterials* **25**, 2393 (2004).
30. A. Horta, M.J. Molina, M.R. Gómez-Antón, and I.F. Piérola: The pH inside a swollen polyelectrolyte gel: poly(N-vinylimidazole). *J. Phys. Chem. B* **112**, 10123 (2008).
31. H.I. Meléndez-Ortiz, C. Alvarez-Lorenzo, A. Concheiro, V.M. Jiménez-Páez, and E. Bucio: Modification of medical grade PVC with N-vinylimidazole to obtain bactericidal surface. *Radiat. Phys. Chem.* **119**, 37 (2016).

https://doi.org/10.1557/mrc.2017.121 Published online by Cambridge University Press